In situ polymerization of tetraethoxysilane in poly(methyl methacrylate): morphology and dynamic mechanical properties

Christine J. T. Landry* and Bradley K. Coltrain
Corporate Research Laboratories, Eastman Kodak Company, Rochester, New York 14650-2110, USA

and Brian K. Brady
Photographic Research Laboratories, Eastman Kodak Company, Rochester, New York 14650-2116, USA
(Received 20 November 1990; accepted 26 February 1991)

Dynamic mechanical spectroscopy and transmission electron microscopy were utilized to investigate the properties of composites resulting from the formation of a cross-linked inorganic network via the polymerization of tetraethoxysilane (TEOS) *in situ* in a poly(methyl methacrylate) (PMMA) binder. The results show that the morphology and physical properties obtained are governed by sample preparation and by the catalyst used to polymerize the TEOS; major differences are obtained when the polymerization of TEOS is performed in different pH regimes. The morphologies which develop are consistent with the known differences in gel structures obtained during the polymerization of TEOS in acidic or basic media. When TEOS is reacted under acidic conditions at elevated temperatures, small (<100 Å) SiO_2 domains which are well dispersed in the PMMA matrix result, producing a composite material with a high plateau modulus above the T_g of PMMA which extends to at least 250°C. The time–temperature–transformation concept, proposed by Gillham for thermosetting organic polymers, is employed to explain some of these results.

(Keywords: morphology; dynamic mechanical properties; polymerization; composite; tetraethoxysilane)

INTRODUCTION

Tetraethoxysilane (TEOS) and other inorganic alkoxides have been used extensively in the sol–gel process to produce monolithic glasses from low temperature processes[1–10]. The network-forming polymerization of the alkoxide, for example TEOS, can be broken down into two principal steps: hydrolysis and condensation.

Hydrolysis: $Si(OR)_4 + nH_2O \rightarrow Si(OR)_{4-n} + nROH$

Condensation:

$$\equiv Si\text{–}OH + RO\text{–}Si\equiv \rightarrow \equiv Si\text{–}O\text{–}Si\equiv + ROH$$

or

$$\equiv Si\text{–}OH + HO\text{–}Si\equiv \rightarrow \equiv Si\text{–}O\text{–}Si\equiv + H_2O$$

These reactions are concurrent and show some reversibility. The relative rates of each are governed by pH, solvent, water to alkoxide ratio, concentration, catalyst, and temperature[11–24]. Therefore, each of these factors plays an important role in the gelation process.

The sol–gel process has been utilized[25–35] to incorporate these highly cross-linked inorganic networks into organic polymeric matrices. This can be accomplished by reacting the orthosilicate directly with reactive end-capped organic polymers or oligomers, thus providing connectivity between the organic phase and the inorganic network which is formed, by precipitation of reinforcing SiO_2 *in situ* into swollen elastomers, or by the hydrolysis and condensation of alkoxysilane monomers containing a polymerizable organic moiety covalently attached to the silicon and the subsequent polymerization of the organic moiety. Alternatively, the *in situ* polymerization can be used in systems with no designed cross-links, producing a microcomposite. This has been done by *in situ* polymerization of titanium alkoxides in poly(*n*-butyl methacrylate)[31] or of silicon alkoxide in perfluorinated ionomer membranes[32]. This combination of organic polymer with inorganic glass can reduce the brittleness of pure inorganic glasses which could help prevent stress cracking during the curing process. Stress cracking severely limits the range of applications for which the sol–gel process can be used, making the fabrication of large monolithic glasses and thick self-supporting films difficult. Silica (SiO_2) filled polymers are used in many commercial applications. The silica acts as a reinforcing agent, imparting increased hardness, compressive strength, heat distortion temperature, plateau modulus and lower thermal expansion coefficient to the polymer[36]. Important factors in determining to what extent these properties are enhanced are filler concentration, shape and the adhesion between the silica and the organic polymer. Mark[29] has demonstrated that a higher modulus and enhanced toughness could be obtained when the reinforcing particles are synthesized *in situ* in poly(methylphenyl siloxane) via the sol–gel process.

* To whom correspondence should be addressed

0032-3861/92/071486-10

The present study represents one phase in ongoing research designed to elucidate the benefits of polymerizing metal alkoxides *in situ* in a polymeric environment. The particular system studied herein consists of the *in situ* polymerization of TEOS in a glassy polymer, poly(methyl methacrylate) (PMMA). The fact that the glass transition temperature, T_g, of the polymer matrix is above ambient temperature introduces a new variable which will affect the polymerization of TEOS, that is, the competition between the rate of vitrification of the system and the rate of inorganic network formation. Also, variables such as pH, solvent, and catalyst will affect the miscibility of the components during the polymerization. All of these factors, starting materials, reaction conditions and processing conditions, will determine the ultimate morphology and physical properties of the composites. Since there is no designed connectivity between the organic (PMMA) and inorganic (SiO_2) phases, interactions between these become critical. The importance of this work lies in the ease of introducing glass reinforcement into the polymeric material, and the ability to control the resulting morphology (SiO_2 particle size and dispersion), thus controlling the ultimate properties of the composite.

EXPERIMENTAL

Materials

The poly(methyl methacrylate) was Plexiglas V(811)-100 from Rohm and Haas Co. and has a $\bar{M}_w = 79\,000$ g mol^{-1} and a $\bar{M}_n = 44\,000$ g mol^{-1} (in polystyrene equivalents) as determined by size exclusion chromatography in THF. The alkoxide used was tetraethoxysilane (TEOS) which was obtained from Fluka Co. The solvent was THF which was reagent grade and was obtained from J. T. Baker, Inc. All reagents and solvents were used as received unless otherwise noted.

All samples were prepared by dissolution of the PMMA in THF at a concentration of 20 wt%. TEOS was added directly to the solution under continuous agitation. The TEOS was well dispersed and the solution became clear within a few minutes. Then a stoichiometric amount of water per alkoxide (4 moles based on Si), either as 0.15 M HCl or 1 M NH_4OH, was added, and the solution was mixed for 16 h at ambient temperature. The solutions were then knife coated onto sheets of Kapton-H mounted on a temperature controlled coating block. All coatings were dried and cured under vacuum at elevated temperatures. The exact conditions used to prepare samples for dynamic mechanical analysis and electron microscopy are listed in *Table 1*.

The nomenclature adopted herein specifies each sample as follows:

PMMA-33A-30 (-90), where

- (-90) is the temperature of highest cure, in °C (not always included in the sample name)
- 30 is the coating temperature, in °C
- A for acid catalysed, B for base catalysed
- 33 mol% TEOS, based on moles of MMA monomer unit
- PMMA organic polymer

Therefore, a sample prepared by adding an amount of TEOS equal in weight to that of PMMA would result in a film containing 33 mol% TEOS (or 33 mol% SiO_2); this is equivalent to 13.5 volume% SiO_2, assuming total conversion of the TEOS to SiO_2 and a density of 2.2 g cm^{-3} for the silica. This density value is used only as a convenience since it is known that, at these cure temperatures, the inorganic phase is not fully densified.

Samples with varying amounts of TEOS were prepared as above; these were all acid catalysed. The coating temperature was varied for several 50/50 (w/w) mixtures of PMMA/TEOS. Also, a few base catalysed samples were prepared for which the time between adding the water/catalyst mixture and solution coating was varied. PMMA-33B-30a was coated immediately after the addition of 1 M NH_4OH, PMMA-33B-30b was coated after 1.5 h, and PMMA-33B-30c was coated after 3 h. All samples are listed in *Table 1*, where PMMA-33B-30 was coated after 16 h as described above.

Table 1 PMMA/TEOS sample composition and preparation

Sample	Composition: Mol % TEOS[a]	Composition: Vol % SiO_2[b]	Catalyst	Coating temperature (°C)	Appearance
PMMA-33B-30	33	13.5	1 M NH_4OH	30	White
PMMA-33B-30	33	13.5	1 M NH_4OH	30	White
PMMA-33B-30a	33	13.5	1 M NH_4OH	30	White
PMMA-33B-30b	33	13.5	1 M NH_4OH	30	White
PMMA-33B-30c	33	13.5	1 M NH_4OH	30	White
PMMA-53A-30	53	26.7	0.15 M HCl	30	Transparent
PMMA-33A-30	33	13.5	0.15 M HCl	30	Transparent
PMMA-33A-19	33	13.5	0.15 M HCl	19	Opaque
PMMA-33A-11	33	13.5	0.15 M HCl	11	Opaque
PMMA-24A-30	24	9.4	0.15 M HCl	30	Transparent
PMMA-17A-30	17	6.3	0.15 M HCl	30	Transparent
PMMA-11A-30	11	3.8	0.15 M HCl	30	Transparent

[a] Based on moles of MMA monomer
[b] Assuming total conversion of TEOS to SiO_2. Density of SiO_2 = 2.2 g cm^{-3}

Measurements

Differential scanning calorimetry (d.s.c.) was performed with a DuPont 990 thermal analyser, equipped with a data analysis program by Laboratory Micro Systems, Inc. The heating rate used was 20°C min^{-1}. The glass transition temperature, T_g, is taken as the onset in the change in heat capacity with temperature.

Dynamic mechanical measurements (d.m.s.) were obtained using a Rheovibron DDV-II dynamic tensile tester (Toyo Measuring Instruments Ltd, Japan) automated by IMASS, Inc. The data were obtained at frequencies of 1.1, 11.0 and 110.0 Hz, using a heating rate of 1.5°C min^{-1}.

Transmission electron microscopy (TEM) was performed on thin (800–1200 Å) sections using a JEOL JEM 100CX-II (JEOL Ltd, Tokyo, Japan) transmission electron microscope. The final print magnifications were between 7800× and 100000×. The samples were microtomed with an LKB Ultrotome V ultramicrotome (LKB Produkter AB, Sweden) perpendicular to the coating direction so that each image represents a cross-section through the thickness of the film. The intrinsic contrast between the organic polymer and the SiO_2 network was sufficient, and no staining was required.

The third dimension in the shape of the inorganic domains for some samples was obtained by the following procedures. The first involved placing the composite in a centrifuge tube with an excess of toluene to dissolve the PMMA. After several hours, the sample was sonicated for 2 h in a warm water bath and centrifuged for 10–20 min. The toluene was removed and a fresh aliquot of toluene was added to the sample and left overnight. The sonication and centrifugation processes were then repeated, most of the toluene removed, and a drop of the remaining solution – which contained the SiO_2 domains – spotted onto a silicon wafer and dried. The sample was then plasma ashed for a total of 8 min in 2 min intervals with 2 min cool times. (One must recognize that the ashing will affect the extent of condensation of the silicate.) Finally, the sample was coated with 3 nm of gold/palladium and photomicrographed with a JEOL JSM-35C (JEOL Ltd, Tokyo, Japan) scanning electron microscope (SEM).

The second procedure involves cutting the film into four equal size pieces. These were staked and glued together with five minute epoxy. The stack was then embedded in Epon 812 in a pyramid mould as follows. Some Epon was placed on the bottom of the mould, after it had begun to cross-link, the stack was positioned on top of it and the mould was filled with Epon. This procedure allowed the stack to remain flat. After hardening the Epon overnight at 50°C, the resulting plug was mounted in a microtome chuck and sections, parallel to the initial film coating direction, were cut with a diamond knife. The results obtained by this latter method will also verify that the first procedure did not alter the macrostructure of the inorganic domains.

RESULTS

Differential scanning calorimetry and dynamic mechanical spectroscopy

The d.s.c. and d.m.s. results indicate that the T_g of the material is not greatly changed by the presence of the inorganic phase. The principal effect on the observed

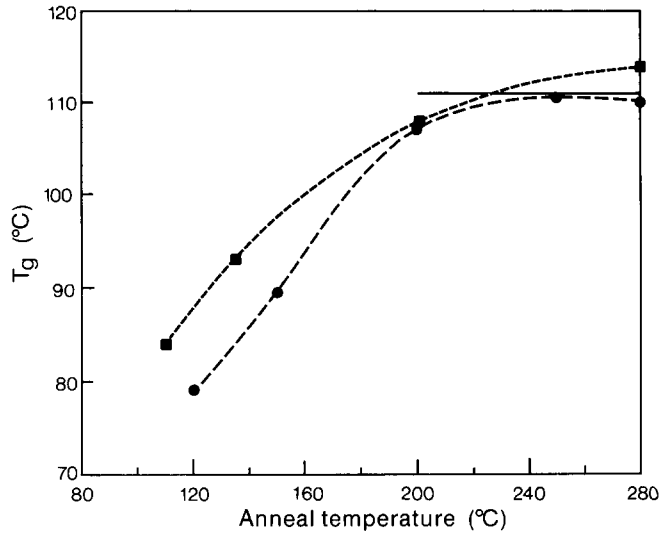

Figure 1 Dependence of T_g, obtained from d.s.c. measurements at 20°C min^{-1}, on annealing temperature. (●) Sample PMMA-33B-30, (■) sample PMMA-33A-30, and the solid horizontal line represents the T_g of PMMA

behaviour of T_g is one of initial plasticization of the PMMA by residual small molecules from the sol–gel reaction: moieties with very low degrees of polymerization such as monomers and dimers. This indicates incomplete curing of the inorganic phase. *Figure 1* illustrates a typical example of the dependence of T_g on cure conditions where curing was performed in the d.s.c. under a nitrogen atmosphere. The exact values for T_g will, of course, depend on the complete thermal history: coating conditions, drying and curing. The T_g of the material can be increased towards its limiting value by curing at elevated temperatures. For this particular system, annealing the sample above 130°C for a sufficient amount of time also leads to a value of T_g which approaches this limiting value. The limiting value is very close to that of PMMA for the base catalysed composite and is slightly higher, by about 7°C, for the acid catalysed composite. The breadths of the d.s.c. transition and the tan δ alpha peak are broader for the TEOS-containing PMMA than for pure PMMA, particularly in the case of the acid catalysed samples.

The dynamic mechanical spectra obtained for samples PMMA-33A-30 and PMMA-33B-30 are shown in *Figure 2*; both samples have been cured for 5 days at 90°C under vacuum. These are compared to the spectrum of pure PMMA. Below T_g the curves for the different samples are all very similar. There seems to be some extra loss near −100°C for the PMMA/TEOS samples, particularly for the acid catalysed system; no explanation for this observation is offered at this time. The β peak, characteristic of PMMA, has the same shape for all three samples although in the case of the base catalysed system the proximity of the glass transition peak to the β peak distorts the shape of the latter. The T_g of both composite samples is slightly depressed relative to pure PMMA, with the base catalysed sample having the lowest T_g.

These samples were analysed for residual volatiles by head space gas chromatography; the incubation was performed at 150°C. The results show that on a relative scale the base catalysed sample contained several wt% residual TEOS, whereas the acid catalysed sample had less than 50 ppm. This is consistent with the known pH

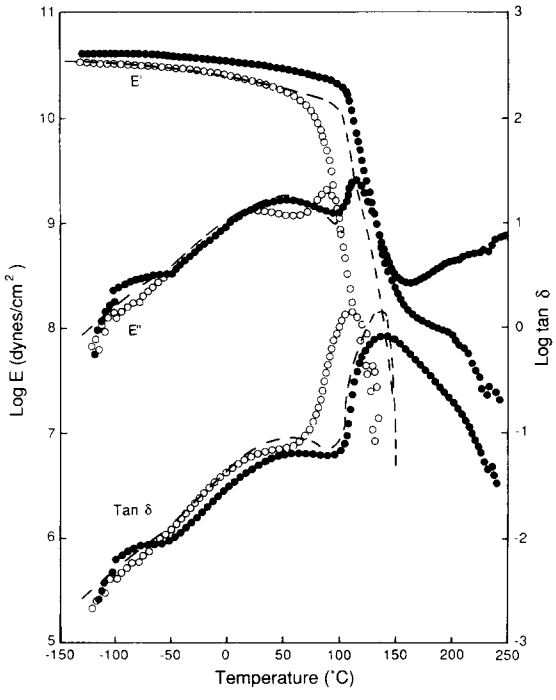

Figure 2 Comparison of the d.m.s. results, at 11 Hz, for the acid *versus* base catalysed PMMA/TEOS composites. (●) Sample PMMA-33A-30, cured at 90°C for 120 h, (○) sample PMMA-33B-30, cured at 90°C for 120 h, and (--) PMMA

effects on the hydrolysis and condensation reactions of silicon alkoxides. This point will be addressed later in the discussion. Additionally, the head space chromatography results indicated that there is a few wt% THF remaining in this acid catalysed sample. No residual solvent was detected in the base catalysed sample. Raman studies confirm these observations.

The predominant difference in the dynamic mechanical behaviour of the two composites was the presence of a rubber-like plateau at temperatures above T_g, having a tensile modulus of log $E' > 8.5$ dynes cm^{-2}, for the acid catalysed composite, whereas the base catalysed sample enters the flow regime after going through T_g. Sample PMMA-33B-30a, coated immediately after the addition of the base catalyst, also entered the flow regime after passing through T_g. The most striking difference in the visual appearance of these samples was optical clarity; the base catalysed sample was opaque whereas the acid catalysed sample was optically clear, suggesting the presence of much smaller silicon oxide domains in the latter.

The acid catalysed composites were usually prepared in such a way as to obtain optically clear films. This is accomplished by coating the solution on a temperature controlled block maintained at, or above, 30°C. If the temperature of the coating block is reduced, cloudy films are obtained. In order to probe differences in morphology and mechanical properties which may arise from varying the sample preparation, samples were coated at 11°C and 19°C (see *Table 1*), keeping all other conditions constant. Their dynamic mechanical properties were obtained and are presented in *Figure 3*. No plateau modulus above T_g is observed for the opaque samples, although the E' curve for the sample cast at 19°C has a slight hint of the beginning of a plateau. Only the clear sample, cast at 30°C shows a plateau modulus. All these samples were cured at 90°C for 2.5 days and have essentially the same T_g. Further curing of the opaque samples increases the T_g but does not promote the development of a rubber plateau. The shift in T_g for the sample cast at 11°C after further curing at 160°C for 2.5 days is also shown in *Figure 3*. For this composite, the maximum in the tan δ curve, at 11 Hz, occurs at 147°C. This is slightly higher than that for pure PMMA, which occurs at 140°C.

Samples of varying TEOS content, coated at 30°C, were analysed by d.m.s. All films were optically clear. The results are shown in *Figures 4* and *5*. For compositions containing 40 wt% (or 24 mol%) TEOS or less, no rubbery plateau was observed. The tan δ peaks, however, were broader than that of pure PMMA. A rubber plateau above T_g is also observed for the composite prepared with 53 mol% TEOS, sample PMMA-53A-30. For this sample, cured at 90°C for 63 h under vacuum, the magnitude of the plateau modulus did not differ from that observed for the sample prepared with 33 mol% TEOS, cured under the same conditions. However, as observed for PMMA-33A-30, the plateau modulus distinctly increased in magnitude as the temperature increased. It was possible to obtain d.m.s. results on sample PMMA-53A-30 after it had been heated to 200°C although the material became extremely brittle after this treatment. These results are also shown in *Figure 5*. The value of the plateau modulus has increased to 10^9 dynes cm^{-2}. These results are evidence that the increase in E' with temperature, above T_g, is at least partially due to further curing of the material. The maximum in the tan δ peak has shifted to about 160°C; this value is also obtained when the sample is cured at

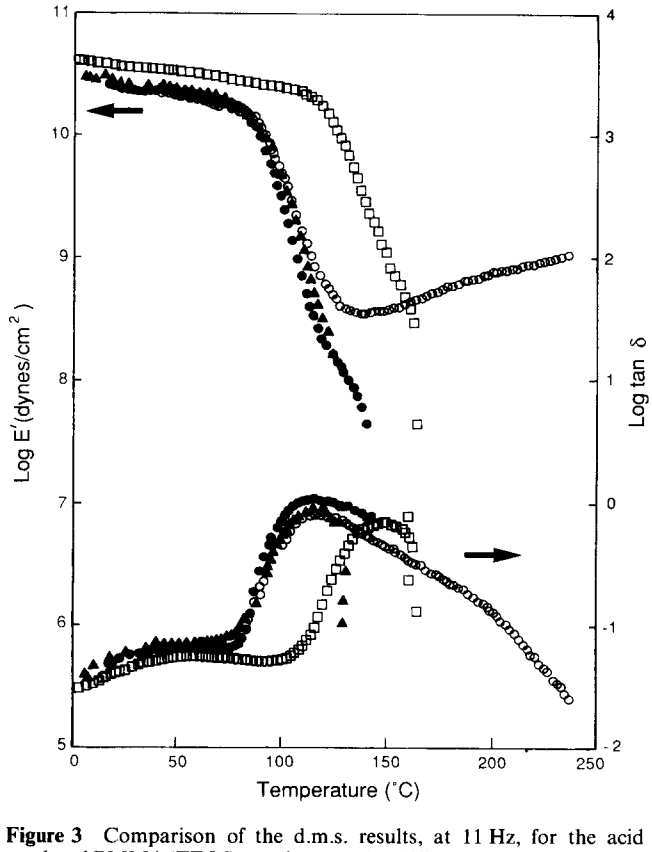

Figure 3 Comparison of the d.m.s. results, at 11 Hz, for the acid catalysed PMMA/TEOS samples coated at different temperatures. (○) PMMA-33A-30, cured at 90°C for 63 h, (●) PMMA-33A-19, cured at 90°C for 63 h, (▲) PMMA-33A-11, cured at 90°C for 63 h, and (□) PMMA-33A-11, cured at 160°C for 65 h

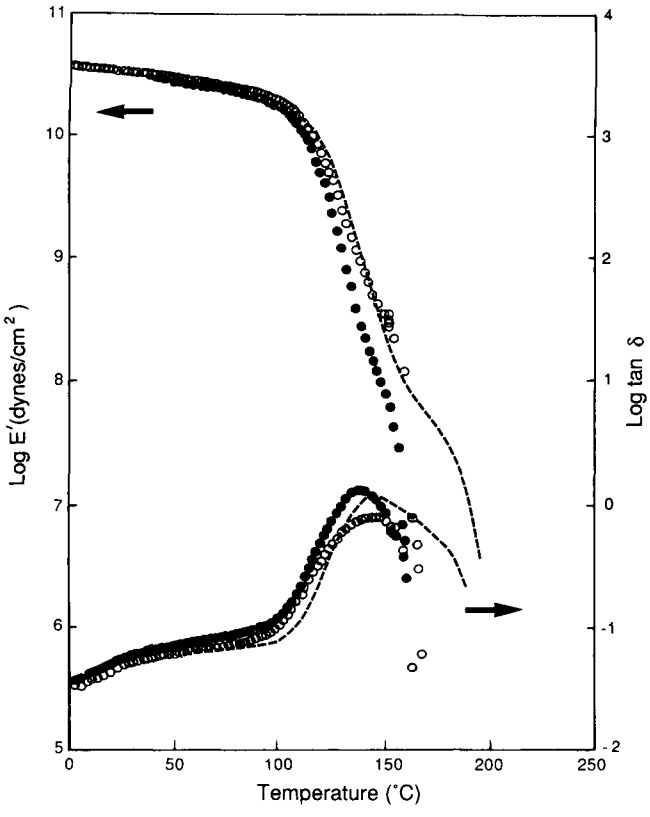

Figure 4 Comparison of the d.m.s. results, at 11 Hz, for the acid catalysed PMMA/TEOS samples of different compositions; all samples were coated at 30°C and cured at 130°C. (●) PMMA-11A-30, (--) PMMA-17A-30, and (○) PMMA-24A-30

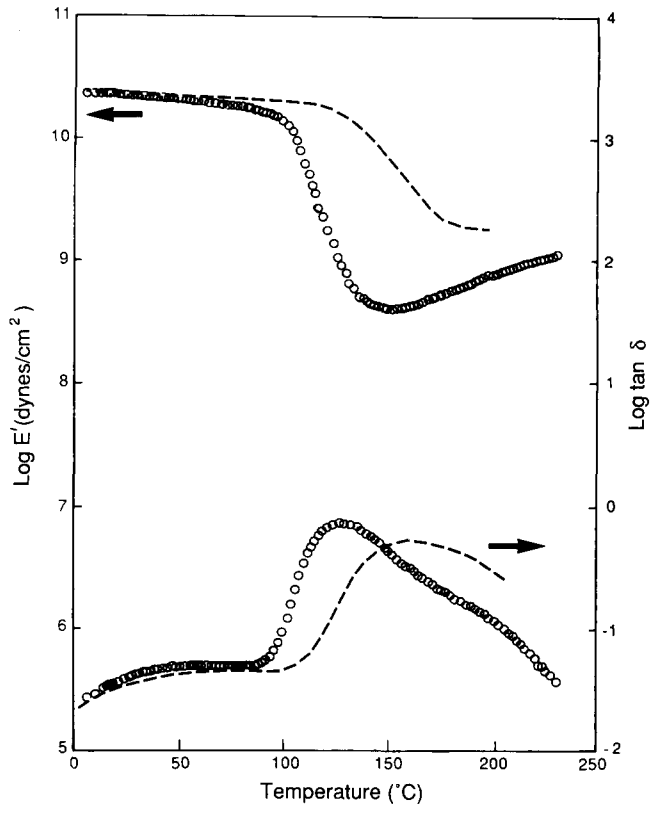

Figure 5 Effect of cure temperature on the d.m.s. results, at 11 Hz, of the acid catalysed sample containing 53 mol% TEOS, sample PMMA-53A-30. (○) Cured at 90°C for 63 h, and (--) cured at 200°C for 30 min

Table 2 D.m.s. results on PMMA/TEOS samples

Sample	Cure conditions T (°C)/time (h)	Tan δ, max T (°C) 11 Hz	Peak height of tan δ, max 11 Hz	Log (plateau modulus) dyn cm^{-2}
PMMA	150/12	140	1.6	–
PMMA-33B-30	90/120	110	1.3	–
PMMA-33B-30a	90/97	130	1.4	–
PMMA-53A-30	90/63	128	0.7	8.6–9.0
PMMA-53A-30	130/65	156	0.5	8.6–9.0
PMMA-53A-30	200/0.5	160	0.3	~9.0
PMMA-33A-30	90/63	117	0.8	8.5–9.0
PMMA-33A-30	90/120	138	0.7	8.4–8.9
PMMA-33A-19	90/63	116	1.0	–
PMMA-33A-11	90/63	117	0.9	–
PMMA-33A-11	160/65	147	0.67	–
PMMA-24A-30	130/18	147	0.75	–
PMMA-17A-30	130/96	147	1.0	–
PMMA-17A-30	90/63	117	1.0	–
PMMA-11A-30	130/15	139	1.2	–

130°C. The amplitude of the loss peak decreases as a function of cure.

The loss peak at the glass transition provides molecular information about the heterogeneity of the system. The tan δ peak is quite sharp for pure PMMA. However, when TEOS is added and polymerized, the breadth of the peak increases. This is particularly pronounced for the acid catalysed samples. Also, the magnitude of tan δ at the peak decreases with SiO_2 content and with extent of cure for the acid catalysed samples. These results are tabulated in *Table 2*. This decrease in peak height is much less pronounced for the base catalysed samples. These results suggest that PMMA is predominantly present as a pure phase in the base catalysed composites, and thus, a more phase separated system is produced than in the optically transparent acid catalysed composites, where

the motions of the PMMA chains are hindered by their close proximity to the SiO_2 network.

Although samples PMMA-33A-11 and PMMA-33A-19 did not exhibit the presence of a rubber-like plateau above T_g, the breadth and magnitude of the tan δ peaks associated with the T_g of these materials have the same characteristics as did samples PMMA-33A-30 and PMMA-53A-30. This indicates some degree of interpenetration of the PMMA chains with the SiO_2 network.

Electron microscopy

The morphology of the base catalysed system, PMMA-33B-30, as observed by transmission electron microscopy, is illustrated in *Figure 6*, where the dark portions represent the SiO_2 rich phase. Observed are spherically shaped silica domains with diameters on the order of 0.1 μm to 0.2 μm. These particles then aggregate to form clusters which vary in shape and size, and measure 1 to 5 μm in diameter. It is noteworthy to recall at this time that the catalyst was added to the PMMA/TEOS solution 16 h prior to the coating process. Thus, the TEOS was allowed to polymerize and to develop some structure in the solution; this would then influence the morphology developed in the solid state.

The early stages of the polymerization of TEOS under base conditions are illustrated by the morphologies of samples PMMA-33B-30-a, b and c. These were coated 0, 1.5 and 3 h, respectively, after the addition of the NH_4OH. *Figure 7* shows the TEMs for samples PMMA-33B-30a, and c; the results for sample b are similar. The development of small SiO_2 rich domains is apparent. These domains are spherical and are initially on the order of 0.05 μm in diameter, and then grow to 0.1 μm in diameter as the time between the addition of NH_4OH and coating is increased. At these early coating stages the particles are well dispersed, contrary to the morphology shown in *Figure 6* where the 0.1 μm size particles have aggregated to form larger SiO_2 rich domains.

In contrast, the images obtained for PMMA-33A-30 revealed a morphology which was very uniform in PMMA/SiO_2 composition. Since the sample section was on the order of 500 Å thick, and individual SiO_2 domains could not be observed even at the highest magnification (hence, no micrographs of this sample are included in this report), it may be concluded that the inorganic glass domains are most probably smaller than 100 Å. After further curing at 160°C for 65 h, some ripening of the inorganic phase occurred but the SiO_2 particle size remained too small to be resolved. Small angle X-ray scattering (SAXS) was performed on the transparent sample PMMA-33A-30. A monotonic decay in the scattering curve was observed, and the results did not contradict the postulation that the silicon oxide particle size is on the order of 100 Å. However, the interpretation of the results was not straightforward and would be qualitative. Therefore, they were not included in this work. Further work in this area is currently under way.

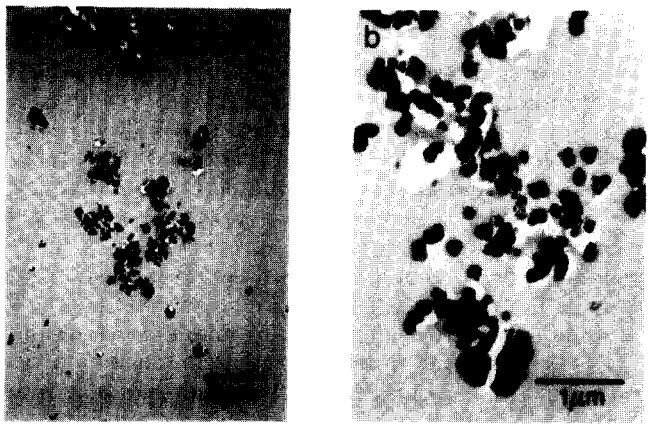

Figure 6 TEM of base catalysed composite PMMA-33B-30 cast 16 h after adding the water

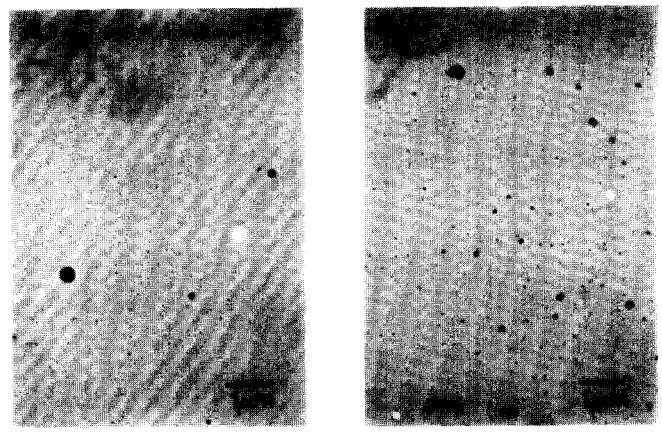

Figure 7 TEM of base catalysed composites: (a) PMMA-33B-30a, cast immediately after adding the water; (b) PMMA-33B-30c, cast 3 h after adding the water

When the acid catalysed systems are coated at temperatures lower than ambient, some interesting changes occur in the development of the final morphology. The micrograph for the PMMA/TEOS sample cast at 11°C, PMMA-33A-11-90, is shown in *Figure 8*. The series of pictures is taken across the thickness of the film, where x is the surface of the sample which was adjacent to the Kapton support, and Y is the surface which was in contact with the air during the drying process at 11°C (*Figure 8a*). The size of the glass domains varies from extremely fine particles, as was observed for PMMA-33A-30, on the air surface, to large, elongated particles on the support side, where the major axis of the particle cross-section is on the order of 1 to 2 μm in length and lies parallel to the film support.

Similar SiO_2 domain shapes and sizes are observed for PMMA-33A-19-90, although the cross-sectional shapes are more uniformly elliptical. No change was observed in the shape and size of the inorganic phase as these samples were cured at 160°C for 2.5 days.

The third dimension of the SiO_2 particle shape was obtained for samples PMMA-33A-11-90 and PMMA-33A-19-90. The SEM results for the first are shown in *Figure 9a* and the TEM results for the second (sectioned parallel to the coating direction) are illustrated by *Figure 9b*. These results are complementary since these two samples have almost identical morphologies. It may therefore be concluded that the SiO_2-rich domains present in the acid catalysed PMMA/TEOS composites coated at low (11°C and 19°C) temperatures are essentially disc shaped particles which lie parallel to the coating surface. These may result from the collapse, in the thickness direction, of spheres.

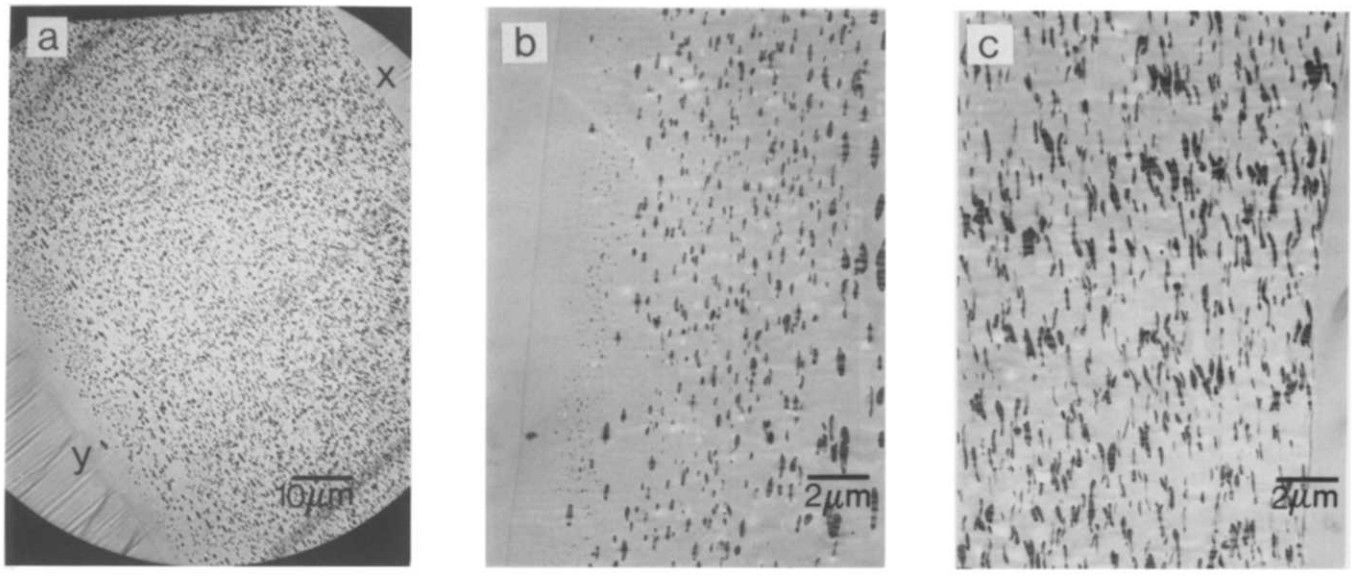

Figure 8 Cross-section of the TEM for acid catalysed composite PMMA-33A-11, cured at 160°C: (a) entire thickness of film where side X is the surface of the coating adjacent to the Kapton support, and side Y is the surface in contact with air; (b) near the air surface; (c) near the Kapton support surface

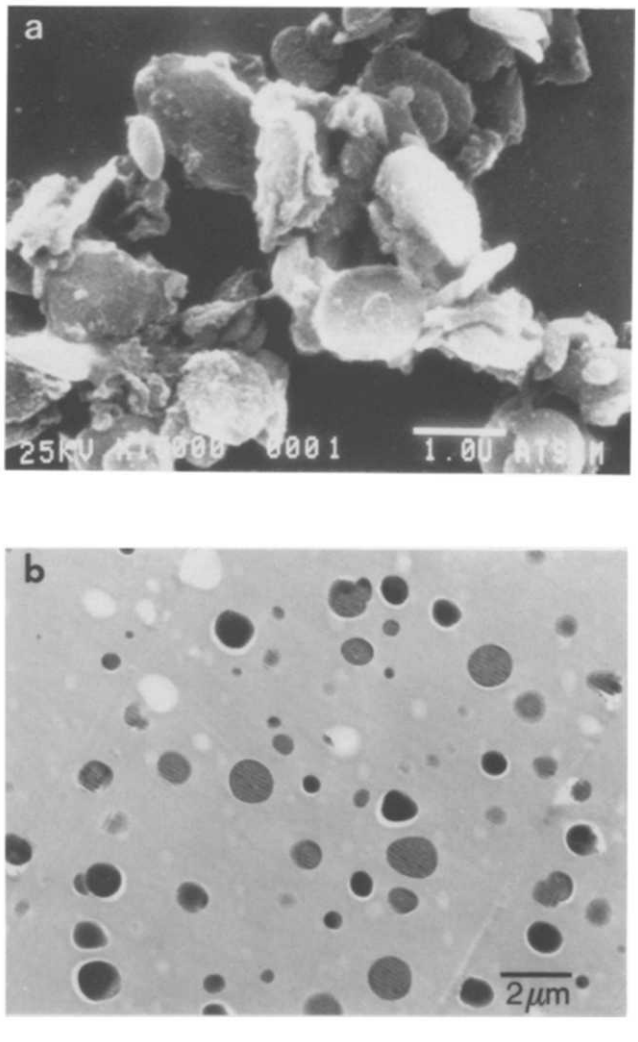

Figure 9 (a) SEM of the extracted inorganic domains present in sample PMMA-33A-11; bar indicates 1 μm; (b) TEM of sample PMMA-33A-19, cross-sectional parallel to the coating direction

DISCUSSION

The lower T_g obtained for base catalysed samples having the same thermal history as the corresponding acid catalysed samples indicates that there are notably more residual low molecular weight species in the former than in the latter. This is supported by head space gas chromatography results which reveal the presence of residual TEOS monomer in the former.

The above results are in agreement with the mechanism of gelation for pure sol–gel reactions under different pH conditions. It has been reported that under acidic conditions hydrolysis is very fast and condensation is the rate determining step. The reverse is generally true under basic conditions[16]. In fact, Kelts *et al.* have shown that very near the gel point for tetramethoxysilane (TMOS) reactions, no unreacted monomer is detected by ^{29}Si n.m.r. at pH* 1, whereas only 26% of the monomers have polymerized under slightly basic conditions[37]. Zerda and co-workers used a molybdic acid reagent to show that at the same stage of the condensation reaction relative to the gel time ($0.3t_g$), virtually all of the silicon atoms are in the polymeric form in acidic media, while only 20–40% are in this form in basic media[17]. Therefore when the film is coated and the system reaches its vitrification point subsequent to solvent evaporation, there may still remain some unhydrolysed TEOS which will no longer be able to react with the inorganic phase, and it would not be surprising to find residual monomer present in the base catalysed systems. We have also ascertained that there remained a few wt% THF in the acid catalysed sample. Both residual monomer and solvent molecules act as plasticizers and suppress the T_g of the samples. It is interesting to note that no residual THF was observed in the corresponding base catalysed sample. This suggests that this composite is a more porous material than the acid catalysed composite.

Samples PMMA-33A-30 and PMMA-33B-30 were prepared identically with the exception of the catalyst.

The morphologies observed by TEM for these samples, in which the TEOS was polymerized *in situ* within the PMMA, are consistent with the known growth mechanism of SiO_2 from TEOS via a sol–gel process. Iler has reported the results of extensive work on the effects of pH on the polymerization of monosilicic acid, $Si(OH)_4$[38]. At low pH there are a large number of nucleation sites due to the rapid hydrolysis which depletes the solution of monomers, and small particles (2–4 nm) are formed. These species can then aggregate, via a cluster–cluster growth mechanism to form oligomers. Polymerization is slow in this pH range so further particle growth is almost negligible. This leads to more open, extended chain-like, ramified structures.

Under basic conditions condensation is rapid, but silica is soluble in this pH regime so monomers are constantly being regenerated by a dissolution process. Silica also has a high negative surface charge under these conditions which suppresses particle aggregation due to electrostatic repulsion. Thus, particle formation proceeds by a monomer-cluster growth mechanism which results in the growth of more compact, highly branched clusters, similar to a nucleation and growth mechanism[38]. Large particles (0.1 μm or larger) are formed by the Ostwald ripening process (where many small particles are transformed into fewer larger particles so as to decrease the total surface energy) and are stabilized by electrostatic repulsion between the particles. The ability to grow micrometre size, monodisperse, spherical SiO_2 particles under basic conditions has been reported in the literature[39].

It would appear that the polymerization of silicon alkoxides is quite similar to the polymerization of monosilicic acid. Pope and Mackenzie[16] have studied the role of the catalyst in the polymerization of TEOS and have shown that the plots of gel time *versus* pH are virtually identical with those reported by Iler for monosilicic acid[38]. Brinker *et al.* have used small angle X-ray scattering (SAXS) to study the polymerization of TEOS under acidic and basic conditions[40,41]. Their results indicated that small, stable particles are produced under low pH conditions where hydrolysis is fast and condensation is relatively slow, whereas larger particles which continued to increase in size were produced at high pH. The particles produced under basic conditions were also noted to be discrete and much more highly condensed than when produced under acidic conditions. However, Brinker and Scherer have reported that solvated polymeric chains, as opposed to dense particles, are produced in both cases, but the base catalysed systems produced more highly branched or collapsed particles[42]. Other workers have presented both Raman and X-ray data to support the observation that much smaller, more ramified polymeric particles are produced under acidic conditions, and larger, more discrete particles are produced under basic conditions[17,18]. Again, the results obtained for the PMMA/TEOS system were entirely consistent with these results reported for the polymerization of silicon alkoxides.

The development of the observed morphology of the PMMA/TEOS composites can be discussed in terms of the well-known phenomenon of vitrification which occurs during cross-linking reactions of thermosetting and high T_g organic polymers. This has been discussed by Gillham in terms of a time–temperature–transformation (TTT) diagram[43]. For the systems described herein, low molecular weight alkoxides are converted to an SiO_2 network. This process is occurring within a polymeric, glassy matrix: PMMA. Initially, the T_g of the system is low due to the presence of solvent molecules which plasticize the polymer, and the polymerization of the inorganic network proceeds rapidly. However, as the solvent evaporates during the coating procedure, the mobility in the system decreases, the T_g increases, and eventually the system vitrifies. Vitrification occurs when the glass transition temperature of the system equals the temperature of cure, T_{cure}. Since the T_g of the fully cured material, T_{ginf}, is above the initial cure temperature (coating temperature), vitrification does occur in these systems, thus retarding further chemical conversion of the inorganic species.

Several processes will be occurring simultaneously, and the morphology developed in a two-phase system will be determined by the relative rates of each process. Domains of one component, SiO_2, grow as a dispersed, and essentially separate, phase since SiO_2 and PMMA are not inherently miscible. The reaction temperature will establish the relative balance between thermodynamic and kinetic factors. This also affects the rate of solvent evaporation. These determine the composition and distribution of dimensions of the dispersed phase; the initial cure temperature (coating temperature) will produce a particular morphology, and subsequent curing at moderately higher temperatures will increase the extent of reaction of the inorganic glass without altering the morphology significantly. For most organic polymer systems, full cure is usually obtained by reaction above T_{ginf}. However, pure SiO_2 will not be obtained until the temperature is raised to above 500°C; this would result in the degradation of PMMA.

The electron micrographs clearly show that the growth mechanism is different in the acid *versus* base catalysed systems. Monitoring the phase separation which occurs in the PMMA matrix is an indirect method of observing this growth process, since it is effectively quenched through vitrification at an intermediate stage of development.

For the acid catalysed composites coated at elevated temperature, the rate of solvent evaporation is high, and the SiO_2 chains do not have time to grow to very high molecular weight prior to vitrification. Thus, phase separation is minimal and we have seen from the increase in the breadth of the tan δ peaks that there is some molecular mixing of the PMMA chains and the SiO_2 network. In the case of the base catalysed PMMA/TEOS sample PMMA-33B-30, the inorganic species have had sufficient time to start their initial growth into isolated SiO_2 particles which may aggregate into colloidal suspensions prior to solution coating. Phase separation occurs rapidly as soon as the film is cast and before the system has a chance to vitrify, thus resulting in micrometre size particles dispersed in the PMMA matrix. The growth of these particles is then followed indirectly by the micrographs shown for samples PMMA-33B-30a, b, c, and PMMA-33B-30.

During a solution coating process a solvent concentration gradient will develop through the thickness of the film; there will be a depletion layer at the surface which is in contact with the air. Thus, the effective T_g of the sample will be higher at the air interface than at the support interface where there is a higher concentration of solvent molecules. This is a result of the fact that

whereas the solvent remains trapped near the bottom of the film, the solvent leaves the air surface rapidly. This creates a deficiency in solvent in that region which then drives the solvent from the bottom surface towards the top. The net result for this system is that the glass precursors which are near the substrate remain mobile for a longer period of time before vitrification, and therefore have time to grow to larger particles. The initial cure of finite specimens throughout which there may be a gradient in solvent concentration, as in the acid catalysed systems which were cast below room temperature, will result in one side vitrifying before the other. This leads to SiO_2 domains which vary in size through the thickness of the film, as shown in *Figure 8*, where the larger SiO_2 particles formed near the substrate. No attempt was made at this time to eliminate this concentration gradient.

The formation of disc-like SiO_2 domains lying parallel to the support in samples PMMA-33A-11 and PMMA-33A-19 is tentatively explained below. In acidic media, TEOS polymerizes to form extended ramified structures. It is possible that these polymers would adopt a somewhat spherical configuration in solution similar to that adopted by the base catalysed systems. However, in the acid catalysed case the individual spheres would be much smaller and much less densely cross-linked. Upon coating and drying, the films shrink a great deal due to solvent evaporation, but the relative shrinkage is greater in the direction perpendicular to the substrate since adhesive forces between the substrate and coating restricts shrinkage in the other dimensions. Since the particles produced in the acid catalysed case are not highly densified, the silicic acid polymer chains can collapse during the shrinkage resulting in the observed disc shaped morphology. The decrease in the tan δ peak height which was observed for these samples could be rationalized in a number of ways. If, as speculated above, the observed disc-shaped morphologies of the SiO_2 domains are due to the collapse of the silicic acid polymer chains during shrinkage, some PMMA chains could be entrapped in the process. High temperature curing will further densify the SiO_2 network, possibly further constraining the PMMA chains. The difference in the tan δ peaks for acid *versus* base catalysed samples indicates a stronger degree of interaction between the inorganic phase and the PMMA chains in the former.

The observation of a high modulus rubber plateau for the hot cast, acid catalysed composites containing at least 33 mol% SiO_2 suggests that there is strong adhesion between the polymer and silica surfaces, where the concentration of residual hydroxide groups is likely to be high at low pH. The latter then act as physical cross-links. Hydrogen bonding often occurs between polymers and hydroxylated silica at low pH. At higher pH, the silica surface retains a sufficient concentration of ionic charges to inhibit the hydrogen bonding[38]. This latter phenomenon probably occurs in the base catalysed samples, which phase separate during the polymerization of the TEOS. This is particularly notable for sample PMMA-33B-30-a which was coated immediately after introducing the water/catalyst mixture. The interaction which results in the uniform composites at low *p*H must also have a stabilizing effect between PMMA and the growing SiO_2 chain throughout the polymerization of TEOS, thus retarding the phase separation of the SiO_2 into large, isolated, regions. The question of hydrogen bonding in the PMMA/TEOS composites will be pursued in more depth in a future report[44].

The magnitude of the observed plateau modulus is on the order of 10^9 dynes cm^{-2} at 250°C. The existence of a rubber plateau in the tensile modulus of a free-standing film above the T_g of the material implies that there is a reinforcing mechanism which persists throughout the sample. This is typically a result of the presence of chemical or physical cross-links, or crystallinity, neither of which are present in these systems. Since the silica domains are very small, the surface area of the particles is extremely large, thus providing many possible interaction sites. For example, SiO_2 particles of 100 Å in diameter will have a surface area of 273 $m^2 g^{-1}$, whereas SiO_2 particles of 0.2 μm in diameter (as observed for the base catalysed composites) would have a surface area of only 14 $m^2 g^{-1}$. These calculations assume spherical, non-porous particles with a density of 2.2 $g cm^{-3}$. Actually, the silica phase is far from being fully densified and the SiO_2 particles are quite porous. Studies[45] of the flocculation of colloidal silica by polymeric materials which hydrogen bond to the silica have shown that the amount of polymer needed to precipitate a given amount of silica was consistent with the following model. When the SiO_2 particles are smaller than about 400 Å, a polymer chain can bridge several particles. Conversely, one or more polymer chains are required to form one contact point between only two larger particles.

If one were to consider these interactions as physical cross-links and apply the known relationship between the magnitude of the rubber plateau modulus and the molecular weight between cross-links[46], one would calculate that there are as few as 10 monomer units between the pseudo cross-links for the acid catalysed composite. This corresponds to a high level of cross-linking.

Although these interactions are probably occurring in all these acid catalysed composites evidenced by the increase in T_g, the increase in the breadth of the damping peak, and the decrease in the magnitude of tan δ, a critical volume % silica seems to be necessary in order to provide the extended pseudo connectivity of the dispersed phase through the entire sample. From the data presented herein, this critical volume % seems to be close to 33 mol% SiO_2 for these composites. Maximizing surface area, however, is not the sole criterion involved; sample PMMA-33B-30a, where the inorganic domains were on the order of 500 Å, did not exhibit a plateau modulus above T_g.

Thus, there are two dominant effects which establish the reinforcing nature of the SiO_2 phase: the concentration of adhesion points between the PMMA and SiO_2 surface, which depends on particle size and concentration, and the chemical character of the surface, which is a function of pH.

CONCLUSIONS

This work has demonstrated that organic polymer properties can be greatly modified by the formation of highly cross-linked inorganic networks via *in situ* polymerization of silicon alkoxides. The polymerization of TEOS in the presence of PMMA produced a composite with a high modulus rubber plateau when the reaction was run under acidic conditions, which generates small

SiO_2 particles well-dispersed throughout the matrix. This mechanical behaviour indicates strong adhesion between the phases. The exact chemical interactions responsible for this adhesion are discussed elsewhere[44]. It is clear, however, that two effects dominate the reinforcing nature of the SiO_2 phase: the concentration of adhesion points between the PMMA and SiO_2 surface, which depends on particle size and concentration, and the chemical character of the surface, which is a function of pH.

It has been shown that the composite morphology and degree of phase separation are extremely important in determining the ultimate material properties, and that these can be controlled with such variables as temperature and pH. It is also clear that T_g is a function of the degree of cure of these materials. Clearly, one must understand the interactions between the competitive processes of polymerization kinetics, phase separation kinetics, and thermodynamics (all of which govern the morphology of the final material) if one hopes to achieve the desired physical properties. It is also key that vitrification be considered as part of the cure cycle in order to optimize properties.

This study provided insight into the interactions between organic polymers and inorganic networks produced *in situ* via a sol–gel process, and into the structure–property relationships of these microcomposites. The methods described herein represent simple means for adding filler particles to organic polymers and producing materials which are easily processed. It was also extremely important to learn that the well-established mechanisms for hydrolysis and condensation of silicon alkoxides in different pH regimes seem to hold when the reactions are done in the presence of an organic polymer. It is hoped that this work can serve as the foundation for the synthesis of novel inorganic/organic materials with designed interactions between the phases which could be used to maximize physical properties.

ACKNOWLEDGEMENT

The authors wish to thank R. O. Gutierrez for his invaluable help with the TEM studies.

REFERENCES

1 Yoldas, B. E. *J. Mater. Sci.* 1979, **14**, 1843
2 Yamane, M., Aso, S., Okano, S. and Sakaino, T. *J. Mater. Sci.* 1979, **14**, 607
3 Klein, L. C. and Garvey, G. J. in 'Ultrastructure Processing of Ceramics, Glasses, and Composites' (Eds. L. L. Hench and D. R. Ulrich), Wiley, New York, 1984, p. 88
4 Beier, W., Gotkas, A. A. and Frischat, G. H. *J. Am. Ceram. Soc.* 1986, **69**, C-148
5 Debsikdar, J. C. *J. Mater. Sci.* 1985, **20**, 4454
6 Zarzycki, J. in 'Ultrastructure Processing of Ceramics, Glasses, and Composites' (Eds. L. L. Hench and D. R. Ulrich), Wiley, New York, 1984, p. 27
7 Hench, L. L. *NATO ASI Ser., Ser. E.* 1985, **92**, 259
8 Orcel, G. and Hench, L. L. in 'Better Ceramics Through Chemistry' (Eds. C. J. Brinker, D. E. Clark, D. R. Ulrich), Materials Research Society, Vol. 32, North-Holland, New York, 1985, p. 79
9 Wallace, S. and Hench, L. L. in 'Better Ceramics Through Chemistry' (Eds. C. J. Brinker, D. E. Clark, D. R. Ulrich), Materials Research Society, Vol. 32, North-Holland, New York, 1985, p. 47
10 Wang, S. H. and Hench, L. L. in 'Better Ceramics Through Chemistry' (Eds. C. J. Brinker, D. E. Clark, D. R. Ulrich), Materials Research Society, Vol, 32, North-Holland, New York, 1985, p. 71
11 Aelion, R., Loebel, A. and Eirich, F. *Am. Chem. Soc. J.* 1950, **72**, 124
12 Aelion, R., Loebel, A. and Eirich, F. *Recueil* 1950, **69**, 61
13 Paoting, Y., Hsiaoming, L. and Yuguang, W. *J. Non-Cryst. Solids* 1982, **52**, 511
14 Nogami, M. and Moriya, Y. *J. Non-Cryst. Solids* 1980, **37**, 191
15 Klein, L. C. and Garvey, G. J. *J. Non-Cryst. Solids* 1980, **38/39**, 45
16 Pope, E. J. A. and Mackenzie, J. D. *J. Non-Cryst. Solids* 1986, **87**, 185
17 Zerda, T. W., Artaki, I. and Jonas, J. *J. Non-Cryst. Solids* 1986, **81**, 365
18 Himmel, B., Gerber, T. and Burger, H. *J. Non-Cryst. Solids* 1987, **91**, 122
19 Yoldas, B. E. *J. Non-Cryst. Solids* 1982, **51**, 105
20 Partlow, D. P. and Yoldas, B. E. *J. Non-Cryst. Solids* 1981, **46**, 153
21 Makherju, S. P. *J. Non-Cryst. Solids* 1980, **42**, 477
22 Yoldas, B. E. *J. Mater. Sci.* 1979, **14**, 1843
23 Brinker, C. J. and Scherer, G. W. *J. Non-Cryst. Solids* 1985, **70**, 301
24 Schaefer, D. W. and Keefer, K. D. *Mater. Res. Soc. Symp. Proc.* 1986, **73**, 277
25 Huang, H.-H. and Wilkes, G. L. *Polym. Bull.* 1987, **18**, 455
26 Huang, H.-H., Orler, B. and Wilkes, G. L. *Polym. Bull.* 1985, **14**, 557
27 Jiang, C.-Y. and Mark, J. E. *Makromol. Chem.* 1984, **185**, 2609
28 Mark, J. E. and Sun, C.-C. *Polym. Bull.* 1987, **18**, 259
29 Clarson, S. J. and Mark, J. E. *Polym. Commun.* 1987, **28**, 249
30 Mauritz, K. A., Jones, C. K. and Warren, R. M. *Polym. Mater. Sci. Eng.* 1988, **58**, 1079
31 Mauritz, K. A. and Jones, C. K. *J. Appl. Polym. Sci.* 1990, **40**, 1401
32 Mauritz, K. A., Storey, R. F. and Jones, C. K. in 'Multiphase Polymers: Blends and Ionomers' ACS Symp. Series 395 (Eds. L. A. Utracki, R. A. Weiss), Washington, DC, 1989, p. 401; Mauritz, K. A. and Warren, R. M. *Macromolecules* 1989, **22**, 1730
33 Philipp, G. and Schmidt, H. *J. Non-Cryst. Solids* 1984, **63**, 283; Schmidt, H. *J. Non-Cryst. Solids* 1985, **73**, 681; Schmidt, H. *Mater. Res. Soc. Symp. Proc.* 1984, **32**, 327
34 Philipp, G. and Schmidt, H. *J. Non-Cryst. Solids* 1986, **82**, 31
35 Mark, J. E., Ning, Y.-P., Jiang, C.-Y., Tang, M.-Y. and Roth, W. C. *Polymer* 1985, **26**, 2069
36 Nielsen, L. E. 'Mechanical Properties of Polymers and Composites' Vol. 2, Marcel Dekker, Inc. New York, 1974
37 Kelts, L. W., Effinger, N. J. and Melpolder, S. M. *J. Non-Cryst. Solids* 1986, **83**, 53
38 Iler, R. K., 'The Chemistry of Silica', Wiley, New York, 1979
39 Stober, W., Fink, A. and Bohn, E. *J. Coll. Interf. Sci.* 1968, **26**, 62
40 Brinker, C. J., Keefer, K. D., Schaefer, D. W. and Ashley, C. S. *J. Non-Cryst. Solids* 1982, **48**, 47
41 Brinker, C. J., Keefer, K. D., Schaefer, D. W., Assink, R. A., Day, B. D. and Ashley, C. S. *J. Non-Cryst. Solids* 1984, **63**, 45
42 Brinker, C. J. and Scherer, G. W. *J. Non-Cryst. Solids* 1985, **70**, 301
43 Gillham, J. K. *Polym. Eng. Sci.* 1986, **26**, 1429
44 Landry, C. J. T., Coltrain, B. K., Wesson, J. A., Zumbulyadis, N. and Lippert, J. L. *Polymer* 1992, **33**, 1496
45 Iler, R. K. *J. Colloid Interface Sci.* 1971, **37**, 364
46 Ferry, J. D. 'Viscoelastic Properties of Polymers', 3rd edition, John Wiley, New York, 1980, Ch. 14